

Electronic Supplementary Information

Ultrasensitive ratiometric fluorescent probe for Hg(II) and trypsin activity based on carbon dots and metalloporphyrin via target recycling amplification strategy

Shan Huang*, Jiandong Yao, Gan Ning, Bo Li, Pingping Mu, Qi Xiao**

Guangxi Key Laboratory of Natural Polymer Chemistry and Physics, College of Chemistry and Materials, Nanning Normal University, Nanning 530001, P. R. China

* Corresponding author. Tel.: +86 771 3908065; Fax: +86 771 3908065;

E-mail address: huangs@whu.edu.cn

** Corresponding author. Tel.: +86 771 3908065; Fax: +86 771 3908065;

E-mail address: qi.xiao@whu.edu.cn

Table S1. Comparison of methods for Hg²⁺ detection

Detection method	Probe	Linear range (nM)	Detection limit (nM)	Sample detection	Reference
Fluorimetry	B-MoS ₂ QDs	5 – 41000	1.8	Environmental water samples	[S1]
Colorimetry	MT-CuNCs	97 – 2300	43.8	Environmental water samples	[S2]
Fluorimetry	N,S-CDs	0 – 40000	2000	Lake water and tap water samples	[S3]
Fluorimetry	Carbonothioate-based far-red fluorescent probe	0 – 1000	3.6	Environmental water samples	[S4]
Electrochemistry	Thiolated graphene	5 – 500	1.1	–	[S5]
Colorimetry	g-C ₃ N ₄ -AuNPs	5 – 500	3	Real water and juice sample	[S6]
Fluorimetry	Au/N-doped CDs	0 – 41860	118	Tap water sample	[S7]
Fluorimetry	Graphitic carbon nitride quantum dots	200 – 21000	3.3	Tap water, lake water, and wastewater samples	[S8]
Fluorimetry	CDs	10 – 1000	2.2	Herbal pills samples	[S9]
Fluorimetry	CDs-based nanohybrid	0 – 40000	9	Human serum and river water samples	[S10]
Fluorimetry	CDs-TPPS ratiometric fluorescent probe	0.2 – 20	0.086	Tap water, lake water, and river water samples	This method

Table S2. Effect of coexisting foreign substances for Hg²⁺ determination (*n* = 3)^a

Foreign substances	Concentration coexisting (μM)	Change of I_{645}/I_{506} (%)	Foreign substances	Concentration coexisting (μM)	Change of I_{645}/I_{506} (%)
L-Lysine	6	-2.56	L-Cysteine	6	+4.80
L-Glycine	6	-3.27	Homocysteine	6	+4.68
L-Glutamate	6	+1.71	Glutathione	6	+4.57
L-Aspartic acid	6	-3.63	Glucose	6	+2.30
L-Phenylalanine	6	-1.30	Fructose	6	-1.30
D-Tryptophan	6	-1.86	Lactose	6	+4.62
L-Tryptophan	6	-3.89	Galactose	6	-3.42
L-Glutathione oxidized	6	+2.23	Maltose	6	+4.02
L-Serine	6	-2.06	AlCl ₃	6	+1.75
L-Arginine	6	-0.96	NiCl ₂	6	-3.04
L-Methionine	6	+4.33	MnSO ₄	6	-4.67
L-Glutamine	6	+3.70	MgCl ₂	6	+0.79
L-Leucine	6	-2.53	CrCl ₃	6	+1.14
L-Valine	6	+3.52	CdCl ₂	6	+4.15
L- α -Alanine	6	+4.38	CaCl ₂	6	-2.38
L-Isoleucine	6	-2.11	NaCl	6	+3.42
L-Asparagine	6	+3.55	BaCl ₂	6	-1.58
L-Histidine	6	+1.02	ZnCl ₂	6	+2.43
Uric acid	6	-4.36	Pb(NO ₃) ₂	6	-3.24
Cholesterol	6	+2.90	CoCl ₂	6	-2.32
Guanosine	6	-4.17	KCl	6	+3.44
Adenosine	6	-3.69			

^a CDs: 17.5 μg/mL; TPPS: 2.5 μM; Hg²⁺: 20 nM; Mn²⁺: 60 nM.

Table S3. Comparison of methods for trypsin activity evaluation.

Detection method	Probe	Linear range (ng/mL)	Detection limit (ng/mL)	Sample detection	Reference
Fluorimetry	BSA-gold nanoclusters	10 – 2000	4	Human urines sample	[S11]
Fluorimetry	Graphene quantum dots-CMR2-BSA	0 – 6000	700	Human urines sample	[S12]
Electrochemistry	Electrochemical probes	5 – 150	1.8	–	[S13]
Colorimetry	Cytochrome c-heme-TMB	5 – 2000	4.5	Human urines sample	[S14]
Fluorimetry	AIZS QDs	200 – 100000	80	Human urine and serum sample	[S15]
Fluorimetry	CuNCs-cytochrome c	0 – 20	2	Human urines sample	[S16]
Fluorimetry	MNP-PDA-HSA composite	500 – 30000	250	Human urines sample	[S17]
Fluorimetry	SDS-protamine-dye	0.01 – 0.1	0.044	–	[S18]
Fluorimetry	Cytochrome c-heme-thiamine	500 – 20000	125	–	[S19]
Chemiluminescence	BSA-AuNCs	10 – 50000	9	Human urines sample	[S20]
Colorimetry	BSA/Au NCs-TMB	900 – 1000000	600	–	[S21]
Fluorimetry	CDs-TPPS ratiometric fluorescent probe	0.1 – 35	0.013	Human urines sample	This method

Table S4. Effect of coexisting foreign substances for trypsin activity evaluation ($n = 3$)^a

Foreign substances	Concentration coexisting ($\mu\text{g/mL}$)	Change of I_{645}/I_{506} (%)	Foreign substances	Concentration coexisting ($\mu\text{g/mL}$)	Change of I_{645}/I_{506} (%)
L-Lysine	6	-1.02	L-Cysteine	6	+3.58
L-Glycine	6	-3.26	Homocysteine	6	+4.12
L-Glutamate	6	+0.11	Glutathione	6	+4.76
L-Aspartic acid	6	+1.72	Glucose	6	+2.27
L-Phenylalanine	6	-3.23	Fructose	6	-0.29
D-Tryptophan	6	+4.16	Lactose	6	-2.08
L-Tryptophan	6	+3.64	Galactose	6	+1.16
L-Glutathione oxidized	6	+1.43	Maltose	6	+3.53
L-Serine	6	-1.52	AlCl_3	6	-1.90
L-Arginine	6	+2.81	NiCl_2	6	-1.13
L-Methionine	6	-2.29	MnSO_4	6	+3.30
L-Glutamine	6	-3.17	MgCl_2	6	+2.46
L-Leucine	6	+1.88	CrCl_3	6	-2.48
L-Valine	6	+0.72	CdCl_2	6	+2.69
L- α -Alanine	6	-3.46	CaCl_2	6	+1.43
L-Isoleucine	6	+1.80	NaCl	6	-2.45
L-Asparagine	6	+3.24	BaCl_2	6	+1.16
L-Histidine	6	+2.98	ZnCl_2	6	-2.56
Uric acid	6	-1.77	$\text{Pb}(\text{NO}_3)_2$	6	+1.25
Cholesterol	6	-3.34	CoCl_2	6	+3.91
Guanosine	6	-0.29	KCl	6	-1.02
Adenosine	6	-2.54			

^a CDs: 17.5 $\mu\text{g/mL}$; TPPS: 2.5 μM ; Hg^{2+} : 20 nM; Mn^{2+} : 60 nM; BSA: 3 $\mu\text{g/mL}$; Trypsin: 30 ng/mL.

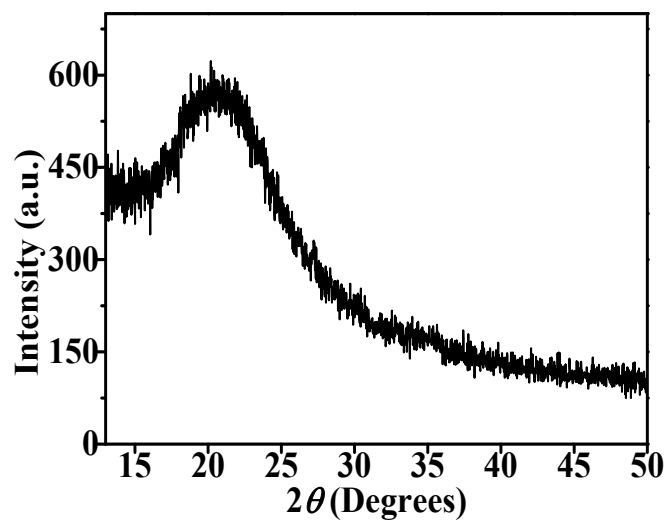


Fig. S1. XRD curve of CDs.

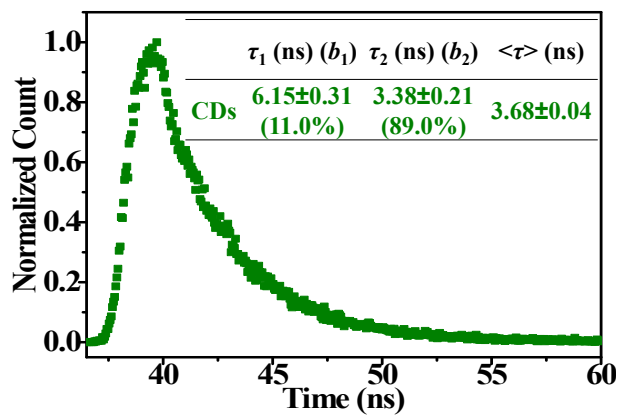


Fig. S2. Fluorescence decay trace of CDs. τ is the fluorescent lifetime of CDs and b is the normalized preexponential factor.

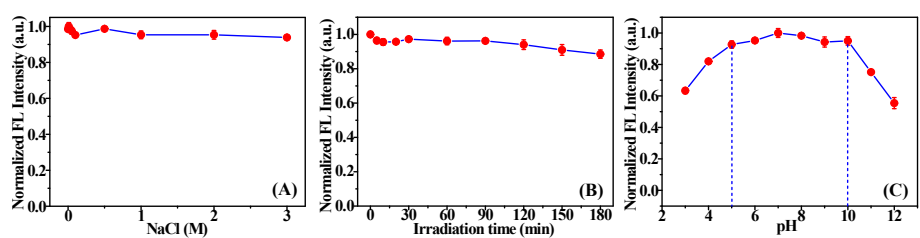


Fig. S3. Influences of the concentration of NaCl (A), irradiation time of 365 nm UV lamp (B), and pH value (C) on the normalized fluorescent intensity of CDs.

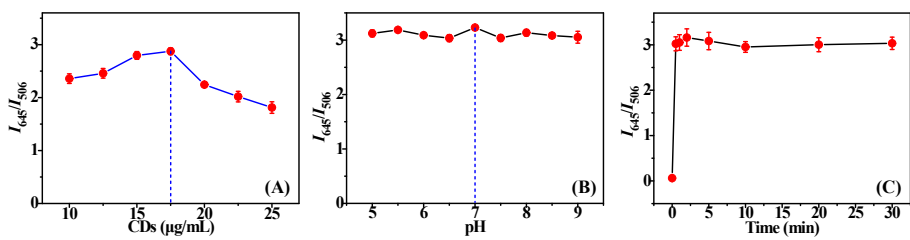


Fig. S4. Influences of the concentration of CDs (A), the pH value of Tris-HCl buffer (B), and the reaction time (C) on the ratiometric fluorescent signal I_{645}/I_{506} . Results were expressed as the average of three independent experiments. Error bars represented the standard deviations.

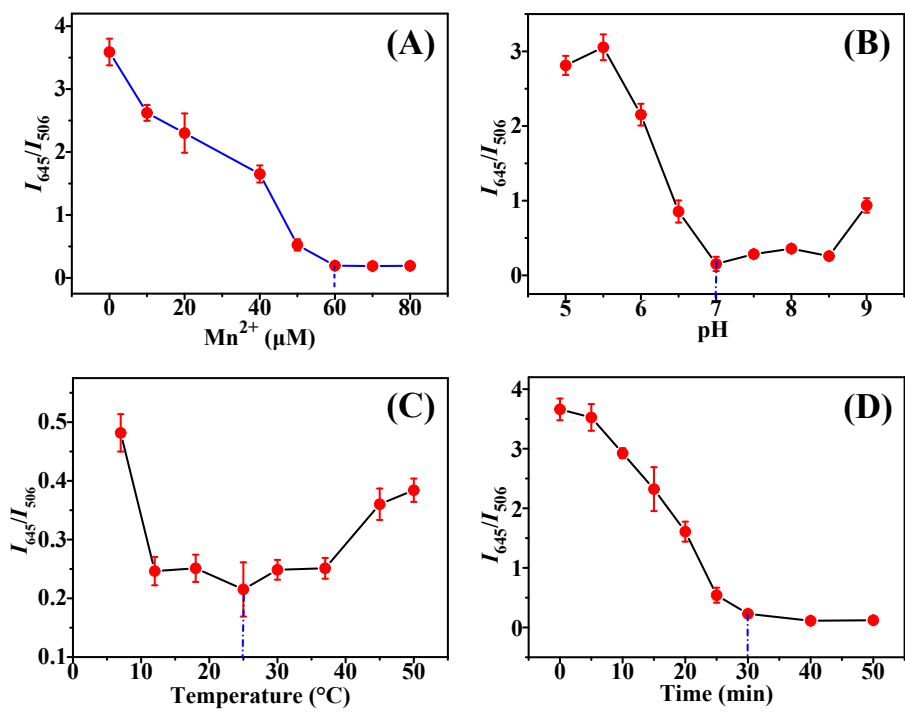


Fig. S5. Influences of the concentration of Mn^{2+} (A), the pH value of Tris-HCl buffer (B), the reaction temperature (C), and the reaction time (D) on the ratiometric fluorescent signal I_{645}/I_{506} . Results were expressed as the average of three independent experiments. Error bars represented the standard deviations.

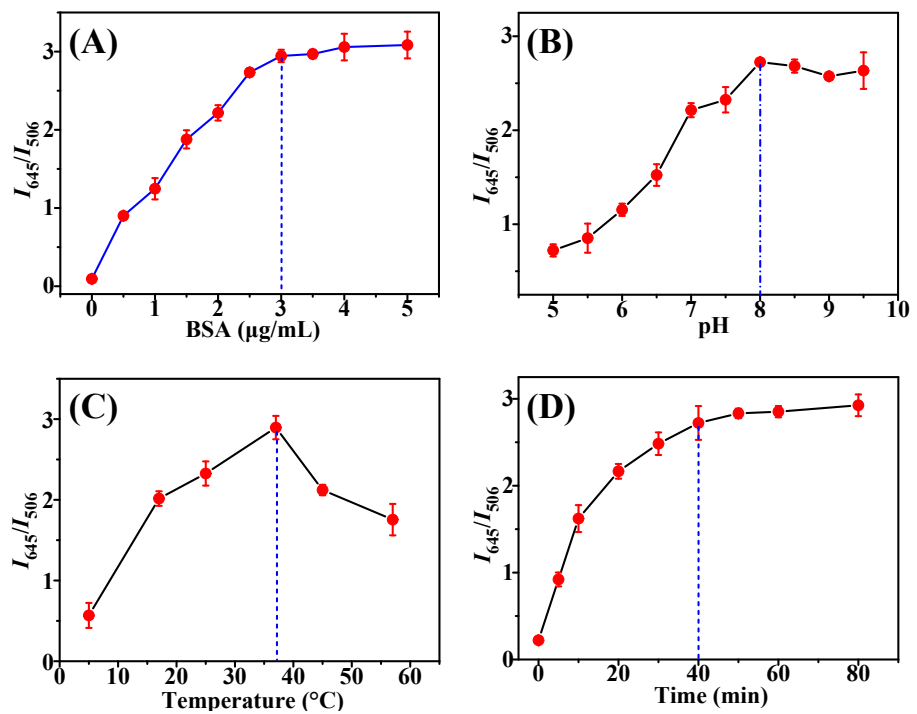


Fig. S6. Influences of the concentration of BSA (A), the pH value of Tris-HCl buffer (B), the reaction temperature (C), and the reaction time (D) on the ratiometric fluorescent signal I_{645}/I_{506} . Results were expressed as the average of three independent experiments. Error bars represented the standard deviations.

References

- [S1] X.R. Guo, J.Z. Huang, Y.B. Wei, Q. Zeng, L.S. Wang, Fast and selective detection of mercury ions in environmental water by paper-based fluorescent sensor using boronic acid functionalized MoS₂ quantum dots, *J. Hazard. Mater.* 381 (2020) 120969. <https://doi.org/10.1016/j.jhazmat.2019.120969>
- [S2] R. Liu, L. Zuo, X.R. Huang, S.M. Liu, G.Y. Yang, S.Y. Li, C.Y. Lv, Colorimetric determination of lead(II) or mercury(II) based on target induced switching of the enzyme-like activity of metallothionein-stabilized copper nanoclusters, *Microchim. Acta* 186 (2019) 250. <https://doi.org/10.1007/s00604-019-3360-6>
- [S3] L.B. Li, B. Yu, T.Y. You, Nitrogen and sulfur co-doped carbon dots for highly selective and sensitive detection of Hg(II) ions, *Biosens. Bioelectron.* 74 (2015) 263–269. <https://doi.org/10.1016/j.bios.2015.06.050>
- [S4] Q.X. Duan, H.C. Zhu, C.Y. Liu, R.F. Yuan, Z.T. Fang, Z.K. Wang, P. Jia, Z.L. Li, W.L. Sheng, B.C. Zhu, A carbonothioate-based far-red fluorescent probe for the specific detection of mercury ions in living cells and zebrafish, *Analyst* 144 (2019) 1426–1432. <https://doi.org/10.1039/C8AN01696H>
- [S5] R. Ziołkowski, A. Uścińska, M. Mazurkiewicz-Pawlicka, A. Małolepszy, E. Malinowska, Directly-thiolated graphene based electrochemical sensor for Hg(II) ion, *Electrochim. Acta* 305 (2019) 329–337. <https://doi.org/10.1016/j.electacta.2019.03.070>
- [S6] Y.W. Wang, Q. Liu, L.X. Wang, S.R. Tang, H.H. Yang, H.B. Song, A colorimetric mercury(II) assay based on the Hg(II)-stimulated peroxidase mimicking activity of a nanocomposite prepared from graphitic carbon nitride and gold nanoparticles, *Microchim. Acta* 186 (2019) 7. <https://doi.org/10.1007/s00604-018-3137-3>
- [S7] A. Meng, Q.H. Xu, K. Zhao, Z.J. Li, J. Liang, Q.D. Li, A highly selective and sensitive “on-off-on” fluorescent probe for detecting Hg(II) based on Au/N-doped carbon quantum dots, *Sens. Actuators B* 255 (2018) 657–665. <https://doi.org/10.1016/j.snb.2017.08.028>
- [S8] X. Wang, X.F. Yang, N. Wang, J.J. Lv, H.J. Wang, M.M.F. Choi, W. Bian, Graphitic carbon nitride quantum dots as an “off-on” fluorescent switch for determination of mercury(II) and sulfide, *Microchim. Acta* 185 (2018) 471. <https://doi.org/10.1007/s00604-018-2994-0>
- [S9] J.H. He, Y.Y. Cheng, T. Yang, H.Y. Zou, C.Z. Huang, Functional preserving carbon dots-

based fluorescent probe for mercury(II) ions sensing in herbal medicines via coordination and electron transfer, *Anal. Chim. Acta* 1035 (2018) 203–210.
<https://doi.org/10.1016/j.aca.2018.06.053>

[S10] J.J. Zhao, M.J. Huang, L.L. Zhang, M.B. Zou, D.X. Chen, Y. Huang, S.L. Zhao, Unique approach to develop carbon dot-based nanohybrid near-infrared ratiometric fluorescent sensor for the detection of mercury ions, *Anal. Chem.* 89 (2017) 8044–8049.
<https://doi.org/10.1021/acs.analchem.7b01443>

[S11] D. Zhao, C.X. Chen, J.H. Zhao, J. Sun, X.R. Yang, Label-free fluorescence turn-on strategy for trypsin activity based on thiolate-protected gold nanoclusters with bovine serum albumin as the substrate, *Sens. Actuators B* 247 (2017) 392–399.
<https://doi.org/10.1016/j.snb.2017.03.031>

[S12] C.Y. Poon, Q.H. Li, J.L. Zhang, Z.P. Li, C. Dong, A.W.M. Lee, W.H. Chan, H.W. Li, FRET-based modified graphene quantum dots for direct trypsin quantification in urine, *Anal. Chim. Acta* 917 (2016) 64–70. <https://doi.org/10.1016/j.aca.2016.02.032>

[S13] R.P. Liang, X.C. Tian, P. Qiu, J.D. Qiu, Multiplexed electrochemical detection of trypsin and chymotrypsin based on distinguishable signal nanoprobes, *Anal. Chem.* 86 (2014) 9256–9263. <https://doi.org/10.1021/ac502318x>

[S14] L.F. Zhang, J.X. Du, A sensitive and label-free trypsin colorimetric sensor with cytochrome c as a substrate, *Biosens. Bioelectron.* 79 (2016) 347–352.
<https://doi.org/10.1016/j.bios.2015.12.070>

[S15] H.X. Li, M.M. Yang, D.S. Kong, R. Jin, X. Zhao, F.M. Liu, X. Yan, Y.H. Lin, G.Y. Lu, Sensitive fluorescence sensor for point-of-care detection of trypsin using glutathione-stabilized gold nanoclusters, *Sens. Actuators B* 282 (2019) 366–372.
<https://doi.org/10.1016/j.snb.2018.11.077>

[S16] S.Y. Zhang, C. Chen, X.F. Qin, Q.C. Zhang, J.H. Liu, J.X. Zhu, Y.Q. Gao, L. Li, W. Huang, Ultrasensitive detection of trypsin activity and inhibitor screening based on the electron transfer between phosphorescence copper nanocluster and cytochrome c, *Talanta* 189 (2018) 92–99. <https://doi.org/10.1016/j.talanta.2018.06.026>

[S17] T.T. Xia, Q. Ma, T.Y. Hu, X.G. Su, A novel magnetic/photoluminescence bifunctional nanohybrid for the determination of trypsin, *Talanta* 170 (2017) 286–290.
S13

<https://doi.org/10.1016/j.talanta.2017.03.081>

- [S18] X. Liu, Y. Li, L. Jia, S. Chen, Y.H. Shen, Ultrasensitive fluorescent detection of trypsin on the basis of surfactant-protamine assembly with tunable emission wavelength, RSC Adv. 6 (2016) 93551–93557. <https://doi.org/10.1039/C6RA19220C>
- [S19] L.F. Zhang, H.Y. Qin, W.W. Cui, Y. Zhou, J.X. Du, Label-free, turn-on fluorescent sensor for trypsin activity assay and inhibitor screening, Talanta 161 (2016) 535–540. <https://doi.org/10.1016/j.talanta.2016.09.011>
- [S20] X.Y. You, Y.H. Li, B.P. Li, J. Ma, Gold nanoclusters-based chemiluminescence resonance energy transfer method for sensitive and label-free detection of trypsin, Talanta 147 (2016) 63–68. <https://doi.org/10.1016/j.talanta.2015.09.033>
- [S21] G.L. Wang, L.Y. Jin, Y.M. Dong, X.M. Wu, Z.J. Li, Intrinsic enzyme mimicking activity of gold nanoclusters upon visible light triggering and its application for colorimetric trypsin detection, Biosens. Bioelectron. 64 (2015) 523–529. <https://doi.org/10.1016/j.bios.2014.09.071>